Hac Thi Nhung

PREPARATION OF FLAME-RETARDANT COMPOSITES BASED ON POLYOLEFIN AND EPOXY USING NANOSTRUCTURED ADDITIVES

**SUMMARY OF DOCTORAL THESIS
IN MATERIALS SCIENCE**

Major: Organic Chemistry

Code: 9 44 01 14

HANOI - 2026

The dissertation is completed at: Graduate University of Science and Technology, Vietnam Academy of Science and Technology

Supervisors:
1. Supervisor 1: Assoc. Prof. Dr. Hoang Mai Ha
2. Supervisor 2: Dr. Le Nhat Thuy Giang

Referee 1:…………………………………..

Referee 2:…………………………………..

Referee 3:…………………………………..

The dissertation is examined by Examination Board of Graduate University of Science and Technology, Vietnam Academy of Science and Technology at ………. o'clock on ………. month ………. year ……….

The dissertation can be found at:
1. Graduate University of Science and Technology Library
2. National Library of Vietnam

LIST OF THE PUBLICATIONS RELATED TO THE DISSERTATION

1. **Investigation of the synergistic effect of red phosphorus and magnesium hydroxide on the thermal degradation behavior and flame resistance of the intumescent fire-retardant polypropylene system**. *Fire and Materials*, 2023, 48(2), 166-179. **Hac T.N.**, Truong C.D., Doan T.D., Ho T.O., Nguyen H.T., Nguyen V.T., Tran Q.V., Hoang M.H.

2. **Two-step preparation of phosphorus-containing organoclay and its effect on fire-resistant and mechanical properties of the flame-retardant polyethylene composite**. *Journal of Applied Polymer Science*, 2024, 141(32), e55758. **Hac T.N.**, Hoang V.T., Truong C.D., Ho T.O., Doan T.D., Nguyen H.T., Le N.T.G., Tran Q.V., Hoang M.H., Nguyen V.T.

3. **DOPO-functionalized Fe-based metal-organic framework and its synergistic flame retardant effect with microencapsulated ammonium polyphosphate in epoxy composites**. *RSC Advances*, 2025, 15, 47587-47600. **Hac T.N.**, Nguyen H.T., Tran D.L., Ho T.O., Doan T.D., Le N.T.G., Nguyen H.T., Nguyen V.T., Hoang M.H.

4. **Preparation of expandable flake-graphite with different particle sizes and their flame-retardant application for polypropylene**. *Vietnam Journal of Science and Technology*, 2024, 62(1), 78-91. **Hac T.N.**, Nguyen T.T.H., Truong C.D., Do T.M.H., Doan T.D., Ho T.O., Nguyen D.T., Hoang M.H.

5. **Haloysit gắn DOPO ứng dụng nâng cao khả năng chống cháy và cơ tính của hệ compozit polyetylen**. *Tạp chí Hóa học & Ứng dụng*, 2024, 3B(71), 166-172. **Hắc Thị Nhung**, Nguyễn Hồng Thắm, Nguyễn Linh Chi, Hồ Thị Oanh, Đoàn Tiến Đạt, Nguyễn Đức Tuyển, Trần Quang Hưng, Trần Quang Vinh, Nguyễn Văn Tuyến, Hoàng Mai Hà.

6. **Synergistic effect of melamine cyanurate, magnesium hydroxide, and red phosphorus on the fire resistance of the intumescent flame-retardant polypropylene composite**. *International scientific conference on current prospects and challenges in chemistry*, 2023. **Hac T.N.**, Truong C.D., Hoang V.T., Doan T.D., Ho T.O., Nguyen D.T., Tran Q.V., Hoang M.H.

7. **Vật liệu compozit chống cháy hiệu năng cao trên nền nhựa polypropylen**. *Thương mại hóa kết quả nghiên cứu: Cơ hội và Giải pháp*, 2025, 325-334. **Hắc Thị Nhung**, Nguyễn Thị Hồng Thắm, Hồ Thị Oanh, Đoàn Tiến Đạt, Nguyễn Thị Thu Hiền, Nguyễn Đức Tuyển, Hoàng Mai Hà.

8. **Dẫn xuất của DOPO và tổ hợp chất chống cháy trên nền epoxy bao gồm dẫn xuất này**. Bằng sáng chế (Đã được chấp nhận đơn hợp lệ)*, Cục sở hữu trí tuệ Việt Nam*, 2024. Nguyễn Văn Tuyến, Trần Quang Hưng, Trần Quang Vinh, Trịnh Đức Công, Hoàng Mai Hà, Nguyễn Linh Chi, **Hắc Thị Nhung**, Đặng Thị Tuyết Anh, Lê Nhật Thùy Giang, Nguyễn Hà Thanh, Nguyễn Thị Quỳnh Giang.

INTRODUCTION

According to statistics from the Fire Prevention, Fighting and Rescue Police Department, during 2020–2024, a total of 14,330 fire incidents occurred nationwide, resulting in 515 fatalities, 551 injuries,and estimated property damage of about 3,116.89 billion VND. In the first six months of 2025 alone, 1,710 fires were recorded, causing 42 deaths, 48 injuries, and estimated losses of 160.98 billion VND. These figures indicate that fires and explosions remain a serious threat, highlighting the urgent need to enhance the fire safety of materials widely used in construction, industry, and daily life

Polymeric materials and composites are increasingly used in construction, industrial, and civil applications due to their versatility and aesthetic advantages. However, most polymers are inherently flammable, exhibiting rapid flame spread, high heat release, and the generation of large amounts of smoke and toxic decomposition products during combustion, which complicate firefighting and rescue operations. In response, Decision No. 630/QD-TTg dated May 11, 2020, issued by the Prime Minister, assigned the Ministry of Science and Technology, in coordination with relevant ministries and agencies, to promote research and development flame retardant materials and extinguishing agents, thereby providing strategic orientation for advancing flame-retardant polymer materials in Vietnam.

In this dissertation, polypropylene (PP), polyethylene (PE), and epoxy resin were selected as research subjects due to their high representativeness in terms of applications and combustion behavior, typifying thermoplastics and thermosets. Differences in their molecular structures and thermal degradation mechanisms impose stringent requirements on flame-retardant systems with high efficiency, good interfacial compatibility, and practical versatility.

Aligned with the trend toward environmentally benign and health-safe flame-retardant systems, this dissertation focuses on the synthesis and surface modification of selected nanostructured materials and inorganic–organic flame-retardant additives. These components are combined to

fabricate flame-retardant composites based on PP, PE, and epoxy matrices. Their flame-retardant performance, mechanical and physical properties, and synergistic mechanisms are systematically investigated. The overall objective is to enhance flame resistance while preserving essential mechanical properties, thereby contributing to the development of safe and efficient flame-retardant polymer materials suitable for practical demands in Vietnam.

Research objectives of the thesis:

This thesis aims to:

❖ Synthesize and modify nanostructured and hybrid materials suitable for application in the preparation of flame-retardant polymer composites.

❖ Surface-modify selected commercial flame retardant additives to improve their compatibility and dispersion within polypropylene (PP), polyethylene (PE), and epoxy matrices.

❖ Develop flame-retardant composites based on polypropylene, polyethylene, and epoxy resins, and optimize the formulation of flame-retardant additives within each polymer matrix to achieve enhanced flame resistance while maintaining satisfactory mechanical performance.

Main research contents:

❖ Content 1: Synthesis and modification of nanostructured materials, including expandable graphite, nanoclay intercalated with phosphorus-containing flame retardants, and metal-organic framework (MOF) materials functionalized with phosphorus-based flame-retardant species.

❖ Content 2: Surface modification of commercial flame-retardant additives, including metal hydroxides, red phosphorus, melamine cyanurate, and ammonium polyphosphate.

❖ Content 3: Preparation of flame-retardant composites based on polyolefins (including polypropylene and polyethylene) and epoxy resins with high flame resistance and good mechanical properties.

Novel Contributions of the Dissertation:

❖ The dissertation has developed two novel flame-retardant nanostructured hybrid materials, including organic nanoclay $oMMT_2$ and MOF–DOPO. These materials simultaneously integrate the gas-phase flame-retardant action of DOPO with the condensed-phase barrier effect and reinforcing characteristics of nanoclay and $Fe-MOF-NH_2$, resulting in high-performance flame-retardant systems.

❖ A solvent-free dry milling method was successfully employed to organically modify the surface of commercial flame-retardant additives. This approach significantly enhanced surface hydrophobicity and reduced particle size, thereby minimizing adverse effects on the mechanical properties of polymer matrices. Moreover, the absence of organic solvents contributes to emission reduction and aligns with sustainable and cleaner production strategies in polymer technology.

❖ The dissertation systematically determined the optimal blending ratios of flame-retardant additives for PP, PE, and epoxy matrices, achieving high flame-retardant efficiency while maintaining mechanical properties suitable for practical applications. In addition, the synergistic flame-retardant mechanisms among the additives were comprehensively analyzed and elucidated, providing deeper insight into their interactive behavior and establishing a scientific basis for the rational design of optimized flame-retardant systems tailored to specific polymer matrices

CHAPTER 1: OVERVIEW

In the Overview chapter, the dissertation presents:

- The theoretical foundations of flame formation mechanisms and the principal mechanisms of action of flame-retardant materials.

- A systematic review of conventional flame retardants, including halogen-containing systems, phosphorus- and/or nitrogen-based flame retardants, intumescent systems, and metal hydroxides, as well as nanostructured materials with flame-retardant capabilities. The review also addresses the

current research status and applications of these flame-retardants in various polymer matrices.

- Overview of the research and development of flame-retardant composites based on polypropylene, polyethylene, and epoxy resins, both internationally and domestically.

- An analysis of the existing limitations and unresolved challenges in previously published studies, thereby identifying research gaps and establishing the scientific orientation and research direction of the dissertation.

CHAPTER 2: EXPERIMENTAL

In the Experimental chapter, the dissertation presents:

- The synthesis and modification procedures for nanostructured and hybrid materials, including expandable graphite, organically modified montmorillonite (oMMT$_2$), Fe-MOF-NH$_2$, and the MOF–DOPO hybrid material.

- The surface treatment methods applied to commercial flame-retardant additives, including aluminum hydroxide, magnesium hydroxide, red phosphorus, melamine cyanurate, and ammonium polyphosphate.

- The preparation procedures for flame-retardant composites based on polypropylene, polyethylene, and epoxy resins.

- The characterization techniques employed to investigate the structural and morphological features of the synthesized nanostructured and hybrid materials, as well as the prepared flame-retardant composites. In addition, the surface properties of the commercial flame retardants after organic treatment were evaluated, together with the flame-retardant performance and mechanical properties of the resulting composite materials.

CHAPTER 3: RESULTS AND DISCUSSION

3.1. RESULTS OF SYNTHESIS AND MODIFICATION OF NANOSTRUCTURED MATERIALS

3.1.1. Synthesis of expandable graphite

Expandable graphite (EG) was synthesized via a chemical intercalation method using flake graphite (FG) with different particle sizes

(+50, +80, +100, +150, and +200 mesh). The increase in interlayer spacing confirmed the successful intercalation and formation of expandable graphite (Fig. 3.1). The expansion volume (EV) was systematically evaluated, and the results indicated that EG derived from +100 mesh FG exhibited the highest expansion capacity, reaching an EV value of 225 mL/g (at 700°C).
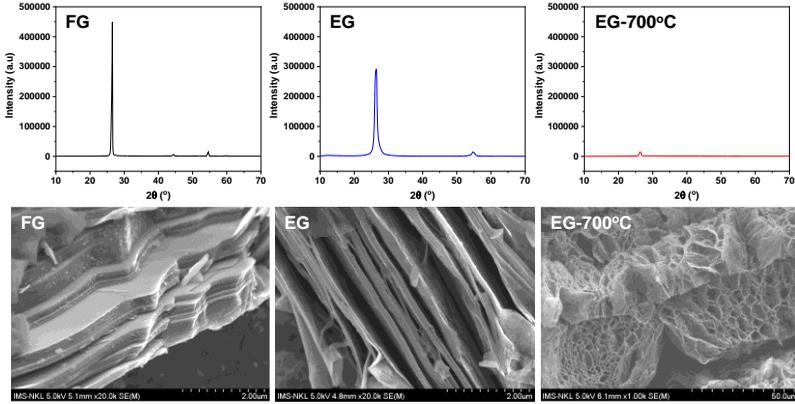

Fig. 3.1. XRD patterns và FE-SEM images of FG, EG và EG heated at 700ºC
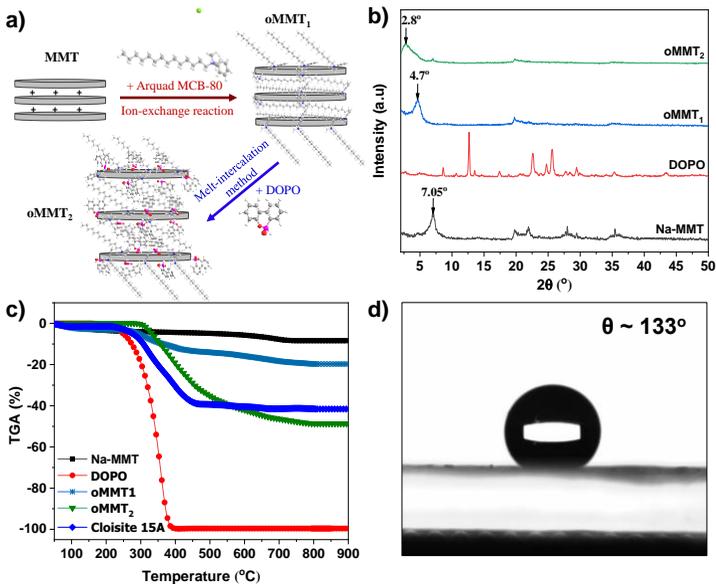
3.1.2. Organic nanoclay

Fig. 3.2. Schematic illustration of the synthesis route of organic nanoclays

(a), XRD patterns (b), TGA curves of Na-MMT, DOPO, and organic nanoclays under N_2 atmosphere (c), and water contact angle of $oMMT_2$ (d)

Organic nanoclay ($oMMT_2$) was synthesized through a combination of ion-exchange and melt-intercalation processes, using Arquad MCB-80 and the phosphorus-containing flame retardant DOPO as intercalating agents (Fig. 3.2a). The resulting $oMMT_2$ exhibited a basal spacing of approximately 31.5 Å. The contents of the intercalated amine and DOPO were determined to be 12.3 wt% and 31.6 wt%, respectively, as calculated from XRD and TGA data (Fig. 3.2b, c). $oMMT_2$ demonstrated pronounced hydrophobicity (Fig. 3.2d), indicating enhanced compatibility with nonpolar organic polymer matrices.

3.1.3. Fe-MOF-NH$_2$ and MOF-DOPO hybrid material

The results of FT-IR, XRD, SEM, and EDS analyses confirmed the successful synthesis of Fe-MOF-NH$_2$ and the MOF–DOPO hybrid material (Fig.3.3). In addition to the characteristic vibrational bands of Fe-MOF-NH$_2$, the MOF–DOPO sample exhibited distinct absorption peaks corresponding to the P–N bond at 1093 and 915 cm^{-1}, indicating the formation of linkages between DOPO the MOF framework.
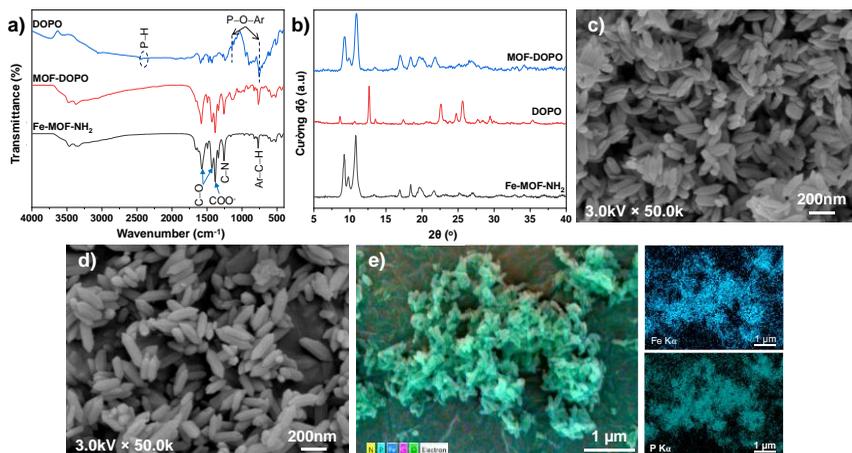

Fig. 3.3. FT-IR spectra (a), XRD patterns (b), FE-SEM images of Fe-MOF-NH$_2$ (c) and MOF-DOPO (d), EDS-mapping of MOF-DOPO (e)

The XRD pattern and FE-SEM image revealed that Fe-MOF-NH$_2$

possesses a rhombic hexagonal crystalline morphology with particle lengths of about 150–235 nm and an average diameter of approximately 60 nm. Importantly, the crystalline structure of the material was preserved after modification. The similarity in the distribution maps of Fe and P elements demonstrated the homogeneous dispersion of phosphorus throughout the MOF crystalline structure, further confirming the successful chemical grating of DOPO to the MOF framework. The P content was determined to be approximately 1.1 wt%, corresponding to a DOPO content of about 7.67 wt% in the modified sample.

3.2. RESUTLS OF SURFACE MODIFICATION OF COMMERCIAL FLAME-RETARDANT ADDITIVES

3.2.1. Surface organic treatment via dry milling

Inorganic flame-retardant additives, including aluminum hydroxide (ATH), magnesium hydroxide (MH), red phosphorus (RP), and melamine cyanurate (MC), were surface-treated by dry milling method using stearate and silane compounds as modifying agents.
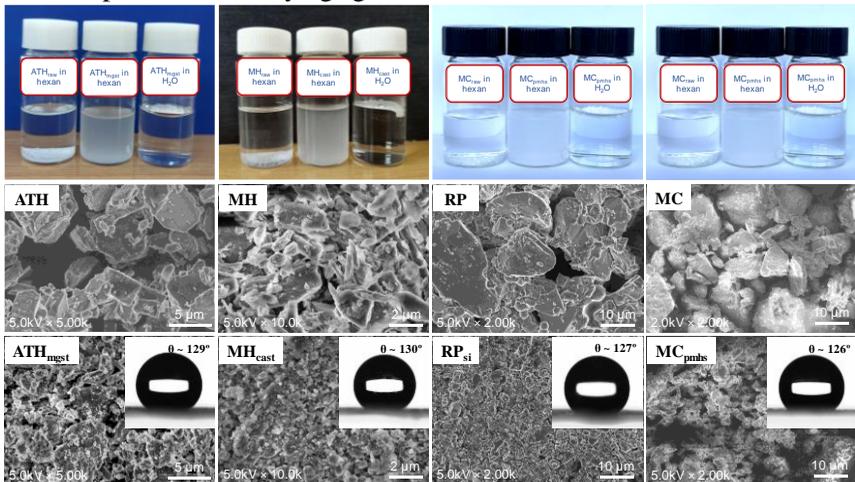

Fig. 3.4. Photographs of surface-untreated and treated additives dispersed in water and hexane; SEM images of the additives before and after surface modification; and water droplets on the surfaces of the modified additives

An optimal loading of 3 wt% magnesium stearate, calcium stearate, silicone oil, and poly(methylhydrosiloxane) was determined for the surface treatment of ATH, MH, RP, and MC, respectively. The modified additives exhibited good dispersion in organic phases with high water contact angle values. SEM observations further revealed that the dry milling process not only enabled effective surface treatment but also significantly reduced the particle size of the additives (Fig. 3.4).

3.2.2. Core–shell structured APP@UMF material

FT-IR spectra, XRD patterns, and SEM images confirmed the successful synthesis of the core–shell structured APP@UMF material (Fig. 3.5). In addition to the characteristic vibrations of ammonium polyphosphate (APP), the FT-IR spectrum of APP@UMF exhibited additional absorption peaks at 1612, 1508, and 600 cm^{-1}, related to the –N–(CO)–N– group, C–N bonds, and triazine ring vibrations, respectively. These features indicate the coexistence of both APP and UMF components within the hybrid material.
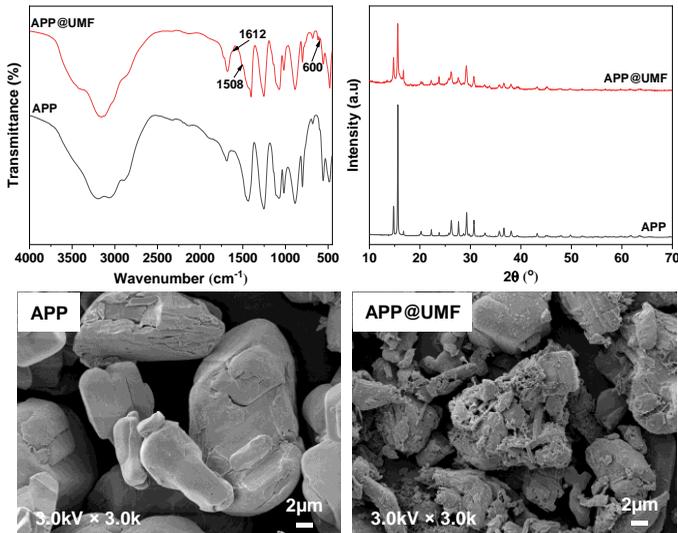

Fig. 3.5. FT-IR spectra, XRD patterns, and FE-SEM images of APP and APP@UMF

The XRD pattern of APP@UMF was similar to that of APP but with

reduced peak intensities, suggesting that the crystalline structure of APP was preserved while being coated with an amorphous UMF layer. SEM observations further corroborated the formation of a well-defined core–shell structure of APP@UMF.

3.3. RESULTS OF PREPARATION OF FLAME-RETARDANT COMPOSITES

3.3.1. Flame-retardant composites based on polypropylene

3.3.1.1. Synergistic effect of melamine cyanurate, red phosphorus, and expandable graphite in PP matrix

■ Flame retardancy

Results of UL94-V and LOI tests (Table 3.1) confirmed the superior flame retardancy of the EG/RP/MC system compared with formulations containing individual additives, demonstrating a clear synergistic effect among the components. The influence of EG particle size on fire resistance was also investigated. The composite containing EG_{100} (PP6) exhibited the highest flame-retardant efficiency, attributed to its larger expansion volume. After formulation optimization, composite PP11 (containing 6.0 wt% EG_{100}, 4.8 wt% RP, and 7.2 wt% MC) achieved a UL-94 V-0 rating and an LOI value of 29.8%, indicating a significant enhancement in the flame resistance of the PP matrix. Improved compatibility and dispersion of the additives within the polymer matrix were also identified as key factors contributing to the enhanced flame retardancy.

Table 3.1. Flame-retardant properties of PP composites

Sample	UL94-V Test				LOI (%)
	$t_1{}^a$ (s)	$t_2{}^b$ (s)	Dripping	Rating	
PP0	Burnt out	-	Yes	N.R.[c]	16.8
PP1	Burnt out	-	Yes	N.R.	20
PP2	Burnt out	-	Yes	N.R.	21.5
PP3	1.0	31.2	Yes	N.R.	23.7
PP4	1.2	16.5	Yes	V-2	25.9
PP5	1.5	1.3	No	V-0	26.8

PP6	1.0	0.6	No	V-0	28.9
PP7	1.7	25.0	Yes	V-2	24.6
PP8	2.1	30.9	Yes	N.R.	24.1
PP9	1.2	1.5	No	V-0	28.1
PP10	1.2	0.7	No	V-0	28.5
PP11	0.4	0.5	No	V-0	29.8
PP12	0.7	0.7	No	V-0	29.1

[a]Self-extinguishing time after the first ignition; [b]Self-extinguishing time after the second ignition; [c]No rating
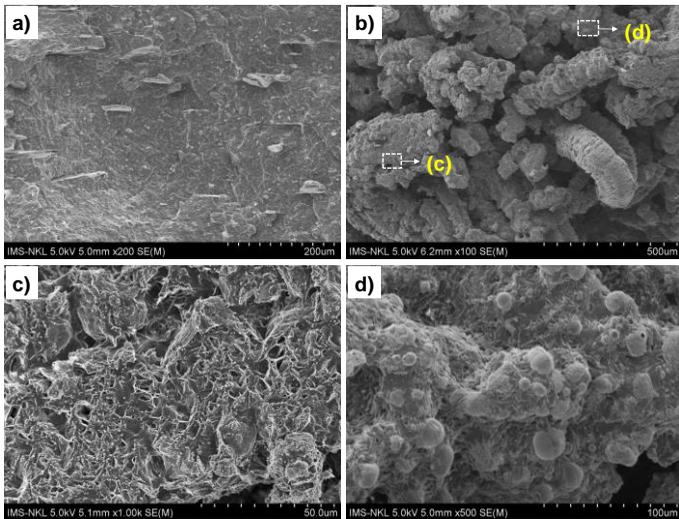

Fig. 3.6. FE-SEM images of PP6 before (a) and after (b-d) the UL94-V test at various magnifications

FE-SEM micrographs of PP6 before and after the UL94-V test (Fig. 3.6) showed that the EG platelets underwent strong expansion upon flame exposure, forming an intumescent char layer that acted as a protective barrier in the condensed phase. However, in a thermoplastic matrix such as PP, melting and dripping during combustion reduced the stability of the char structure formed by EG. The simultaneous presence of MC and RP reinforced and stabilized the

char layer of EG through a synergistic N–P effect, promoting the formation of phosphorus–nitrogen-rich macromolecular structures. As a result, the char layer became more cohesive, compact, and continuous, significantly enhancing the overall flame retardancy of the composite.

■ Thermal behavior

TGA results in air atmosphere (Fig. 3.7) demonstrated that EG, RP, and MC exert distinct effects on the thermal degradation behavior of PP. EG and MC significantly increased the char yield of the composites; however, this char structures exhibited limited stability at elevated temperatures. In contrast, RP markedly improved the thermal stability of the polymer matrix.
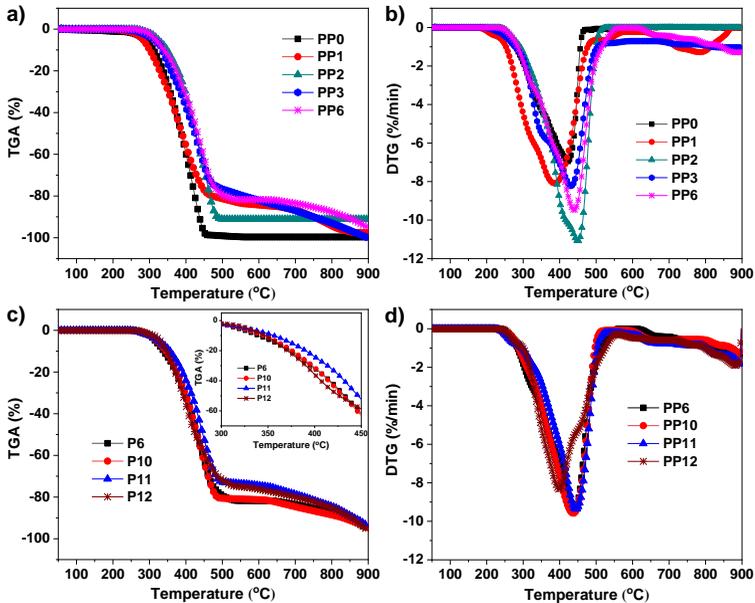

Fig. 3.7. TGA (a, c) và DTG (b, d) curves of composites under air atmosphere

When the combined EG/RP/MC system was employed, composite PP6 showed a pronounced enhancement in thermal stability compared with PP0, with an increase in T_{max} of 15.7°C and an experimental char yield substantially higher than the theoretical value. This improvement is attributed to the formation of thermally stable phosphorus–nitrogen

macromolecular structures, such as $(PNO)_x$ and $(PN)_x$ species, which reinforce and stabilize the EG char layer, thereby effectively suppressing thermo-oxidative degradation. Investigation of the RP/MC ratio revealed that a ratio of 2:3 was optimal, enabling the composite to achieve the highest thermal stability and flame retardancy.

■ Mechanical properties

Overall, the addition of flame-retardant additives led to a reduction in the mechanical properties of the PP matrix. Among the investigated additives, EG exerted the most adverse effect on tensile properties, with the tensile strength and elongation at break of PP1 decreasing by 21.9% and 61.6%, respectively, compared with PP0. In contrast, MC markedly reduced the impact strength from 57.48 to 8.5 kJ/m^2. The combination of flame-retardant additives, together with surface organic modification, significantly mitigated the deterioration in mechanical properties of the composites (Fig. 3.8).
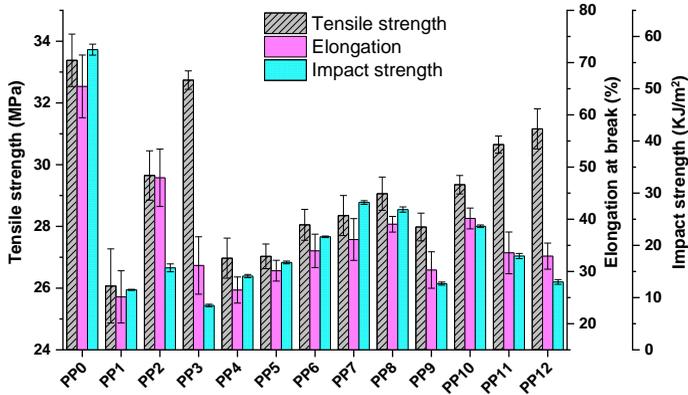

Fig. 3.8. Mechanical properties of PP composites

3.3.1.2. Synergistic effect of magnesium hydroxide, red phosphorus, and expandable graphite in PP matrix

■ Flame retardancy

Results of UL94-V and LOI tests (Table 3.2) proved a pronounced synergistic flame-retardant effect for the MH/RP/EG system, leading to a significant improvement in the flame retardancy of the PP matrix compared with

the use of individual additives at the same total loading. Among the investigated formulations, PP15 (7.2 wt% MH, 4.8 wt% RP, and 6 wt% EG) exhibited the optimal performance, achieving a UL-94 V-0 rating and the highest LOI value of 27.2%. In addition, the surface organic modification of MH and RP contributed to the improved flame-retardant efficiency of the composites.

Table 3.2. Flame-retardant properties of PP composites

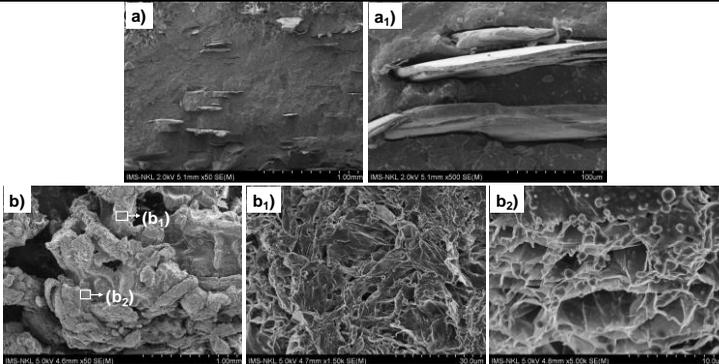| Sample	UL94-V Test				LOI (%)
	t_1 (s)	t_2 (s)	Dripping	Rating	
PP0	Burnt out	-	Yes	N.R.	16.8
PP1	Burnt out	-	Yes	N.R.	20
PP2	Burnt out	-	Yes	N.R.	21.5
PP13	Burnt out	-	Yes	N.R.	19.7
PP14	1.1	1.0	No	V-0	26.8
PP15	0.8	1.0	No	V-0	27.2
PP16	1.0	9.0	No	V-0	25.9
PP17	2.0	50.0	Yes	N.R.	23.2
PP18	1.2	1.8	No	V-0	26.3

Fig. 3.9. FE-SEM images of PP15 before (a, a_1) and after (b, b_1, b_2) the UL94-V test at various magnifications

The surface morphology of PP15 before and after the UL94-V test was observed by SEM (Fig. 3.9). Similar to the phenomenon observed for PP6

(Fig. 3.6), the formation of thermally stable magnesium phosphate species played a crucial role in reinforcing the EG char structure. As a result, the char layer became more compact and robust, thereby markedly enhancing the condensed-phase flame-retardant efficiency of the composite.

■ Thermal behavior

TGA analysis in air also confirmed that the intumescent char of EG was effectively protected from high-temperature oxidation, as evidenced by the nearly constant char residue of PP14 in the 500–900°C range. Investigation of the MH/RP ratio revealed that PP15 exhibited the highest thermal stability. Based on the combined UL-94, LOI, and TGA results, an MH/RP ratio of 3:2 was identified as optimal for achieving both superior flame-retardant performance and enhanced thermo-oxidative stability.
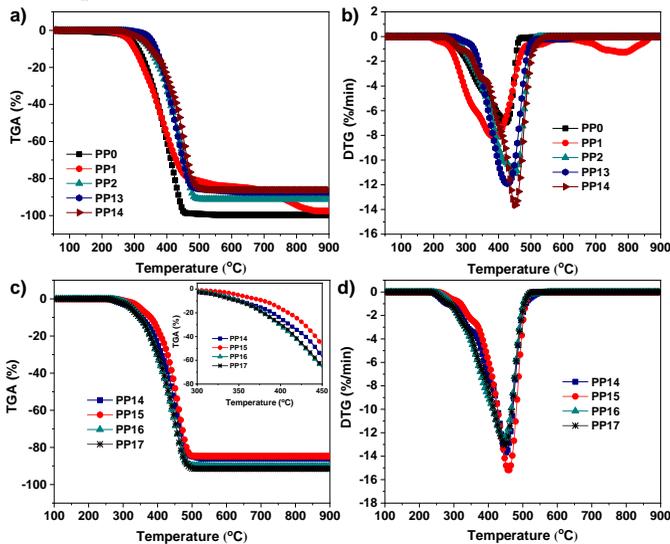

Fig. 3.10. TGA (a, c) và DTG (b, d) curves of the composites in air

■ Composition of char residues at different MH/RP mass ratios

The residues of PP14–PP17 after heating to 900°C were characterized by FT-IR, XRD, and EDS analyses. The results indicated that the char layers consisted of the expanded graphite, MgO, and magnesium phosphate

compounds ($Mg_3(PO_4)_2$, $Mg(PO_3)_2$, and α-$Mg_2P_2O_7$), coexisting in both crystalline and amorphous phases.
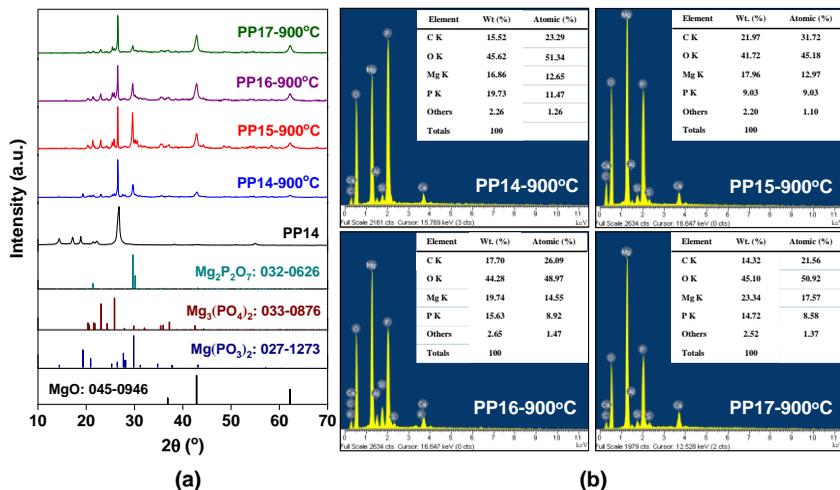

Fig. 3.11. XRD patterns (a) và SEM-EDS spectra (b) of composites before and after heating to 900°C

Notably, PP15 (MH/RP = 3:2) generated the highest content of crystalline magnesium phosphates (52.6 wt%), with α-$Mg_2P_2O_7$ as the dominant phase (~36.7 wt%). In contrast, further increasing the MH/RP ratio led to a decrease in the amount of the crystalline magnesium phosphates accompanied by a significant increase in the content of MgO. These findings highlighted the crucial role of magnesium phosphate species, particularly α-$Mg_2P_2O_7$, in protecting the composite and rationalize the observed trends in flame retardancy.

■ Composition of residue at different temperatures

The interactions among the flame retardants in the PP15 composite were elucidated by FT-IR and XRD analyses after thermal treatment at different temperatures (Fig. 3.12). At 300°C, MH had not undergone decomposition and no phosphate compounds were formed. At 400°C, initial signs of interaction between MH and RP were detected, as evidenced by the formation of a small amount of magnesium pyrophosphate (β-$Mg_2P_2O_7$). In the temperature range of 500–600°C, $Mg(OH)_2$ completely decomposed into

MgO, while magnesium phosphate species continued to form but predominantly existed in the amorphous phase. When the temperature reached ≥700°C, the phosphate phases progressively transformed into thermally stable crystalline forms, including $Mg(PO_3)_2$, $Mg_3(PO_4)_2$, and α-$Mg_2P_2O_7$, reflecting the development and stabilization of the char structure at elevated temperatures.
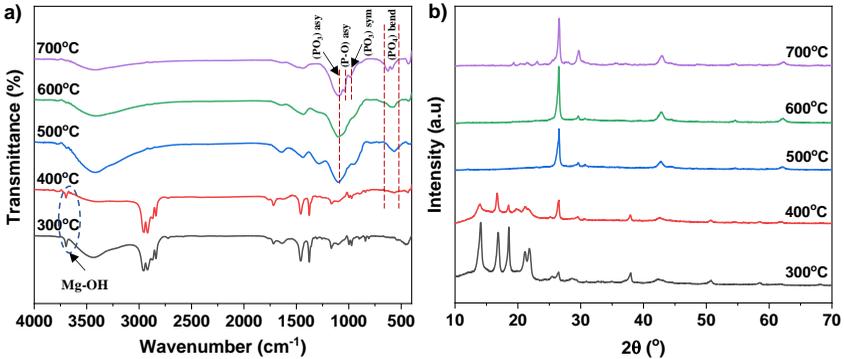

Fig. 3.12. FT-IR spectra (a) và XRD patterns (b) of char residue of PP15 at different temperatures

■ Mechanical properties

Fig. 3.13 presented the mechanical properties of neat PP and its composites. Overall, the incorporation of flame-retardant additives reduced the mechanical performance of the PP matrix; however, MH_{cast} exerted a significantly lower adverse effect compared with EG and RP_{si}. The surface organic modification of MH and RP markedly improved the compatibility and dispersion of the additives, thereby substantially enhancing the mechanical properties of the composites, as evidenced by the simultaneous increases in tensile strength, elongation at break, and impact strength.

Compared with the $EG/RP_{si}/MH_{cast}$ system, the $EG/RP_{si}/MC_{pmhs}$ formulation at the optimal ratio (PP11) exhibited a more pronounced synergistic flame-retardant effect while still maintaining the mechanical properties required for practical applications. Therefore, this system was identified as the optimal flame-retardant formulation for PP composites.
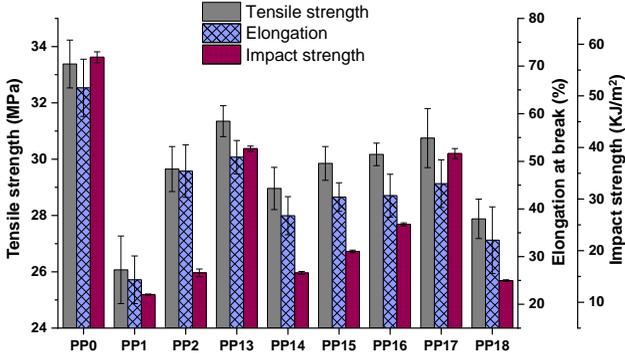
Fig. 3.13. Mechanical properties of PP and its composites

3.3.2. Flame-retardant composites based on polyethylene

3.3.2.1. Flame retardancy

Results of UL94-V and LOI tests (Table 3.3) showed that the incorporation of the ATH/RP system (3:2) significantly improved the flame retardancy of the PE matrix; however, dripping behavior still persisted.

Table 3.3. Flame-retardancy and mechanical properties of PE composites

Sample	UL94-V Test				LOI (%)	Tensile strength (MPa)	Elongation at break (%)
	t_1 (s)	t_2 (s)	Dripping	Rating			
PE0	Burnt out	-	Yes	N.R.	17.5	29.77 ± 0.65	677.44 ± 22
PE1	1.0	2.8	Yes	V-2	25.1	21.68 ± 0.23	480.61 ± 50
PE2	1.2	1.4	No	V-0	26.3	22.96 ± 0.1	578.68 ± 28
PE3	1.0	1.7	Yes	V-2	26.0	22.50 ± 0.5	505.19 ± 15
PE4	0.9	1.0	No	V-0	26.8	23.98 ± 0.15	575.33 ± 25
PE5	0.7	0.7	No	V-0	27.6	24.10 ± 0.2	600.17 ± 20
PE6	1.3	2.5	Yes	V-2	25.4	23.21 ± 0.3	559.11 ± 10

Partial substitution of ATH/RP with $oMMT_2$ markedly enhanced the flame-retardant performance due to a synergistic effect. Meanwhile, the composite containing 3 wt% $oMMT_2$ and 17 wt% ATH/RP achieved the highest fire resistance, with a UL-94 V-0 rating and LOI of 27.6%. However, when the $oMMT_2$ content was further increased, the flame-retardant efficiency of the material gradually decreased.

3.3.2.2. Thermal behavior

TGA results in air (Fig. 3.14) showed that the ATH/RP system significantly enhanced the thermal stability of PE, with the T_{onset} value of PE1 increasing by approximately 63.44°C compared with that of PE0. The incorporation of $oMMT_2$ into the ATH/RP system slightly reduced the thermal stability but markedly increased the char yield of the composites.
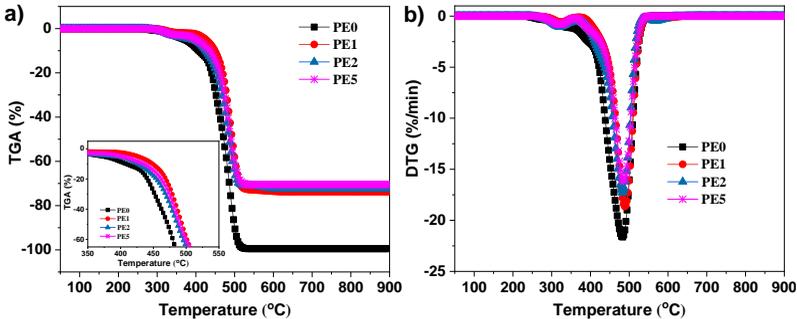

Fig. 3.14. TGA (a) và DTG (b) curves of neat PE and its composite in air

3.3.2.3. Flame-retardant mechanism

The char layer of PE5 after the UL94-V test exhibited a compact and continuous structure, which acted as an effective physical barrier by restricting heat transfer and inhibiting the release of flammable volatile products, thereby suppressing combustion and enhancing the flame retardancy of the material.
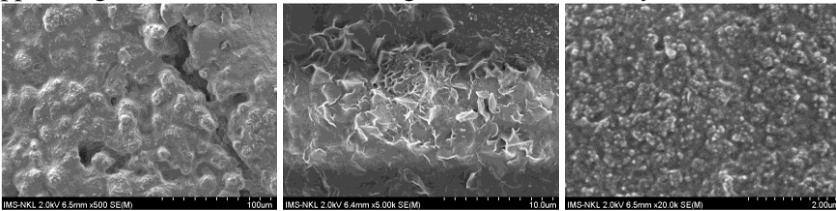

Fig. 3.15. FE-SEM images of the char surface of nanocomposite PE5 after UL94-V test at different magnifications

The flame-retardant mechanism of the nanocomposite involved a synergistic effect between gas and condensed-phase actions (Fig. 3.16). In the gas phase, phosphorus-containing free radicals inhibited flame propagation, while the released water vapor diluted the combustion zone. In the condensed phase, the formation of phosphoric/polyphosphoric acid layers together with

metal phosphate compounds generated an efficient insulating barrier. Notably, the presence of $oMMT_2$ promoted the formation of a silicate-rich char layer with high thermal stability and structural integrity, which significantly improved the overall flame-retardant performance of the material.
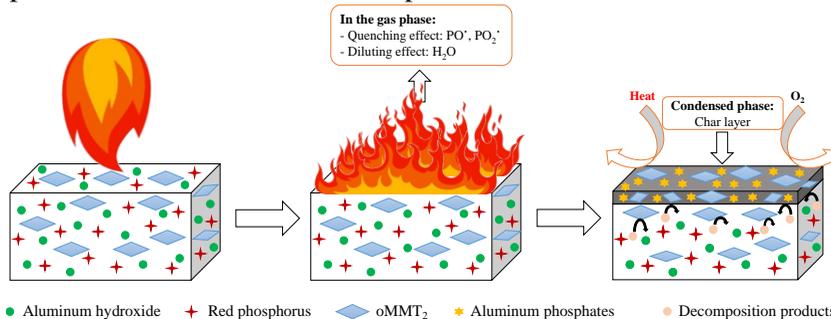

Fig. 3.16. Synergistic flame-retardant mechanism of nanocomposite PE5

3.3.2.4. Mechanical properties

The tension results (Table 3.3) indicated that that the incorporation of the ATH/RP system reduced the tensile properties of the PE matrix, primarily due to the large particle size of these additives. Partial substitution of ATH/RP with low contents of $oMMT_2$ (1–3 wt%) significantly improved the tensile strength and elongation at break of the composite, which was attributed to the effective exfoliation and dispersion of silicate layers within the polymer matrix. PE5 (containing 3 wt% $oMMT_2$ and 17 wt% ATH/RP) exhibited superior mechanical performance, with a tensile strength of 24.10 MPa and an elongation at break of 600.17%.

It was concluded that the combination of 3 wt% $oMMT_2$ and 17 wt% ATH/RP represented the optimal formulation for preparing PE nanocomposites with high flame retardancy, thermal stability, and good mechanical properties.

3.3.3. Flame-retardant composite based on epoxy resin

3.3.3.1. Flame retardancy

In this section, epoxy composites were prepared using Fe-MOF-NH$_2$, MOF-DOPO, and APP@UMF as flame retardants. Results of UL94-V and LOI tests showed that the addition of 10 wt% APP@UMF improved the flame

retardancy of epoxy. When APP@UMF was combined with either Fe-MOF-NH$_2$ or MOF-DOPO, the fire resistance was further enhanced. Notably, MOF-DOPO exhibited superior synergistic flame-retardant performance, indicating the significant role of DOPO functional groups in promoting synergistic interactions. Evaluation of the formulation ratios indicated that EP3 (containing 1 wt% MOF-DOPO and 9 wt% APP@UMF) achieved the optimal flame-retardant performance, attaining a UL-94 V-0 rating with the shortest burning time and the highest LOI value (37.3%). However, further increasing the MOF-DOPO content led to a noticeable decline in the flame retardancy.

Table 3.4. Flame-retardancy and mechanical properties of epoxy composites

Sample	UL94-V Test			LOI (%)	Tensile strength (MPa)	Elastic Modulus (MPa)	Impact strength (KJ/m^2)
	t_1 (s)	t_2 (s)	Rating				
EP0	Burnt out	-	N.R.	21.1	83.69 ± 0.2	1590.64 ± 65	45.92 ± 0.1
EP1	1.2	1.5	V-0	28.5	46.67 ± 0.5	2286.10 ± 90	11.43 ± 0.3
EP2	0.9	1.3	V-0	30.7	54.76 ± 0.8	2190.12 ± 82	16.89 ± 0.2
EP3	0.5	0.6	V-0	37.3	60.95 ± 0.4	2249.71 ± 45	21.12 ± 0.4
EP4	0.8	1.0	V-0	33.8	61.74 ± 0.3	2360.88 ± 30	21.85 ± 0.1
EP5	10.3	2.6	V-1	24.6	59.24 ± 0.6	2373.97 ± 35	19.56 ± 0.3

3.3.3.2. Thermal behavior

Results of TGA under air atmosphere (Fig. 3.17) showed that the incorporation of APP@UMF accelerated the thermal decomposition of the polymer matrix due to the catalytic effect of phosphoric acid derivatives, thereby promoting char formation. When APP@UMF was combined with Fe-MOF-NH$_2$ or MOF-DOPO, the thermo-oxidative stability of the nanocomposites was markedly improved, as evidenced by the increases in T$_{max}$ and char yield. This enhancement was attributed to the catalytic carbonization effect of the metal active sites and the formation of thermally stable metal phosphate species. Among the samples, EP3 exhibited the highest thermal stability, with T$_{max2}$ and T$_{max3}$ reaching 597.25°C and 804.06°C, respectively, along with a high char yield of 17.68%.
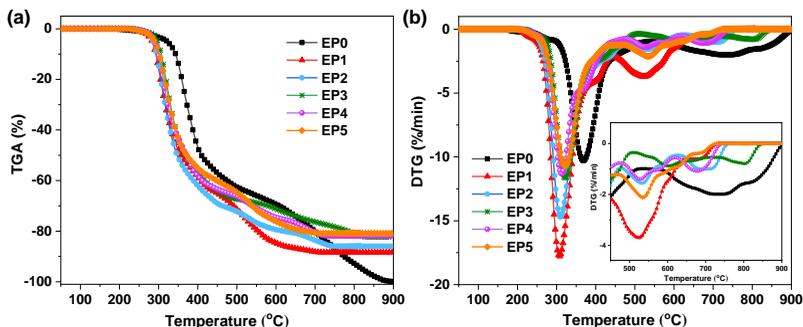
Fig. 3.17. TGA (a) và DTG (b) curves of epoxy and its composites in air

3.3.3.3. Morphology of char residue

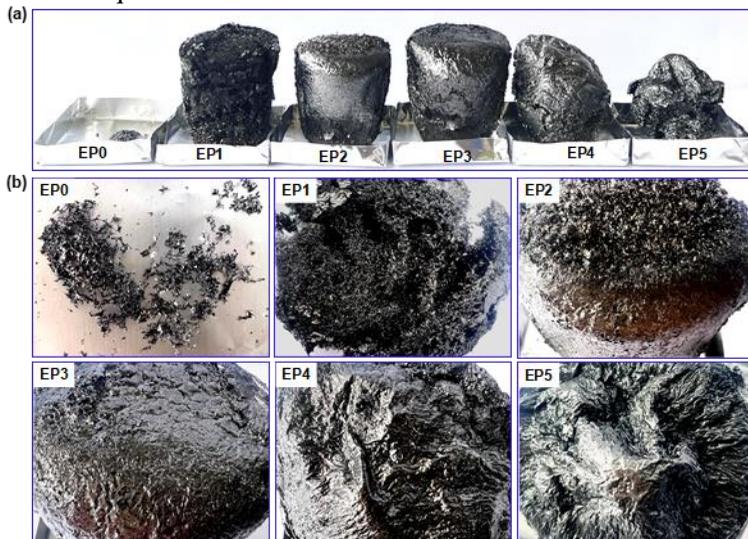Fig. 3.19 displayed the char structures of the composites after calcination at 900°C with equal initial masses.

Fig. 3.19. Digital photographs of EP and its composites obtained after calcination at 900°C: Side view (a) and Top view (b)

The composite containing 10 wt% APP@UMF formed a large-volume intumescent char layer; however, its porous, discontinuous, and mechanically weak structure rendered it susceptible to collapse during combustion. Partial substitution of 1 wt% APP@UMF with MOF or MOF-DOPO reinforced the char structure, resulting in a more robust and

continuous char layer, particularly in the case of MOF-DOPO. However, at higher MOF-DOPO loadings, although the mechanical strength of the char further increased, the degree of expansion decreased markedly.
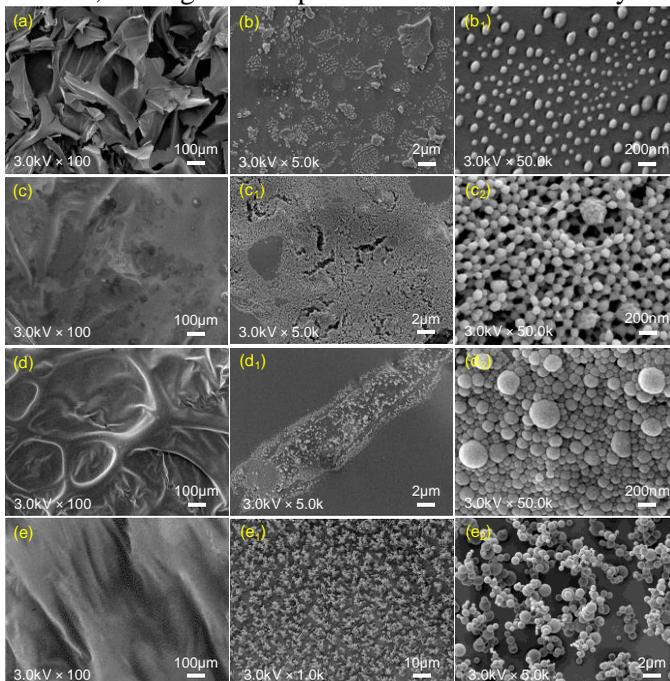

Fig. 3.20. The surface morphology of EP1 (a), EP2 (b, b_1), EP3 (c, c_1, c_2), EP4 (d, d_1, d_2), EP5 (e, e_1, e_2) after calcination at 900°C

FE-SEM images (Fig. 3.20) showed that the char layer of EP1 exhibited a loose, porous, and mechanically weak structure, which limited its flame-retardant effectiveness. In contrast, nanocomposites EP2–EP5 formed denser, more continuous, and more stable char layers. The appearance of a densely distributed network of spherical particles on the char surface reinforced the structure, enhanced its thermal stability, and significantly improved its protective performance. Furthermore, the development of this thermally stable particulate network likely generated a secondary shielding layer that hindered direct flame contact with the underlying matrix, thereby markedly enhancing the protective capability of the char layer.

3.3.3.4. Flame-retardant mechanism

FT-IR and XRD analyses (Fig. 3.21) showed that the char layer of EP1 predominantly consisted of an amorphous phosphorus-rich carbon structure formed through aromatization and carbonization processes. In addition to the phosphorus-rich char framework, nanocomposites EP2–EP5 exhibited the presence of thermally stable iron phosphate species, including $Fe(PO_3)_2$, $Fe_2P_4O_{12}$, $Fe_2P_2O_7$.
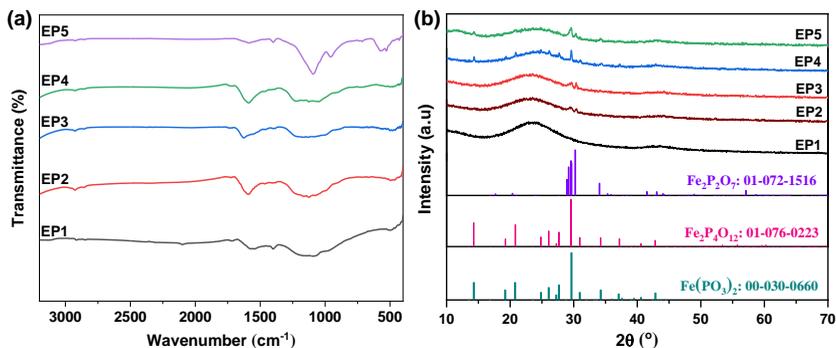

Fig. 3.21. FT-IR spectra (a) and XRD patterns (b) of epoxy composites EP1–EP5 after calcination at 900°C

The synergistic flame-retardant mechanism between MOF-DOPO and APP@UMF in the epoxy matrix involved gas-phase flame inhibition by phosphorus-containing free radicals and non-combustible gases, combined with the formation of an intumescent phosphorus-rich char in the condensed phase. Notably, the development of a metal phosphate particulate network covering the char surface reinforced the char structure and enhanced its thermal shielding efficiency. Among the formulations, the combination of 1 wt% MOF-DOPO and 9 wt% APP@UMF provided the superior flame-retardant efficiency for the epoxy matrix.

3.3.3.5. Mechanical properties

The mechanical test results (Table 3.4) indicated that the incorporation of APP@UMF reduced the tensile strength and impact strength of the epoxy matrix. In contrast, partial substitution of APP@UMF with MOF or MOF-DOPO markedly improved the mechanical performance of the composites

due to improved dispersion and effective reinforcement, particularly in the case of MOF-DOPO.

CONCLUSIONS

The dissertation successfully synthesized nanostructured and hybrid materials, including expandable graphite; $oMMT_2$ organic nanoclay with an interlayer spacing of 31.5 Å, containing 12.3 wt% Arquad MCB-80 and 31.6 wt% DOPO; and MOF-DOPO hybrid material containing 7.67 wt% DOPO. These exhibited well-controlled structures and morphologies, demonstrating the effective integration of phosphorus-based flame-retardant functionality with the barrier and reinforcing features of nanostructured materials.

A green approach for the organic modification of the flame-retardant additives was developed using a dry milling technique with stearate and silane agents, which improved dispersion and compatibility of the additives within polyolefin matrices. Additionally, microencapsulation of APP with a urea–melamine–formaldehyde polymer shell enhanced its dispersion in the epoxy matrix.

Pronounced synergistic flame-retardant effects were demonstrated in specific polymer matrices, and the optimal additive compositions were identified. For PP, the combination of 6.0 wt% EG, 4.8 wt% RP_{si}, and 7.2 wt% MC_{pmhs} achieved UL-94 V-0 and LOI of 29.8%. For PE, the system comprising 3.0 wt% $oMMT_2$, 10.2 wt% ATH_{mgst}, and 6.8 wt% RP_{si} attained UL-94 V-0 and LOI of 27.6%, while maintaining good mechanical properties (tensile strength of 24.10 MPa and elongation at break of 600.17%). For epoxy, the combination of 1 wt% MOF-DOPO and 9 wt% APP@UMF achieved UL-94 V-0 and LOI of 37.3%, while meeting mechanical requirements for practical applications.

The synergistic flame-retardant mechanisms of these additive systems were systematically elucidated through comprehensive analyses of thermal behavior, structural evolution, morphology, and char composition, thereby providing a scientific basis for the design of high-performance flame-retardant polymer composites in future research.